Materials Research Express

PAPER

Development of a new quaternary alloy Ti–25Ta–25Nb–3Sn for biomedical applications

Materials Research Express

RECEIVED
18 July 2017

REVISED
19 August 2017

ACCEPTED FOR PUBLICATION
23 August 2017

PUBLISHED
1 February 2018

PAPER

Development of a new quaternary alloy Ti–25Ta–25Nb–3Sn for biomedical applications

Mauricio Rangel Seixas[1], Celso Bortolini Jr[1], Adelvam Pereira Jr[1], Roberto Z Nakazato[1], Ketul C Popat[2] and Ana Paula Rosifini Alves Claro[1]

[1] UNESP—Universidade Estadual Paulista, School of Engineering, Guaratinguetá Campus, Brazil
[2] Colorado State University, School of Biomedical Engineering, Fort Collins, CO, United States of America

E-mail: rosifini@feg.unesp.br (**A P R Alves Claro**)

Keywords: titanium alloys, mechanical properties, biomedical applications

Abstract

Metallic biomaterials have been used for biomedical applications, such as cardiovascular, orthopaedics and orthodontics, due to excellent properties. In this study, the mechanical properties and corrosion resistance of new quaternary alloy Ti25Ta25Nb3Sn were evaluated. Alloys were processing in arc melting furnace with argon atmosphere and cold worked by rotary swaging. Alloy microstructure, crystalline phases and mechanical properties such as Young's modulus, yield strength and tensile strength were evaluated. Corrosion resistance was investigated in fluoride solution by electrochemical polarization and biocompatibility with human dermal fibroblasts were also evaluated. In our study, for quaternary alloy Ti25Ta25Nb3Sn the stabilization of beta phase was maintained. It was observed that the elastic modulus of Ti25Ta25Nb3Sn (65 GPa) was lower than CP Ti (105 GPa) and Ti6Al4V (110 GPa) and slightly higher than Ti25Ta25Nb (55 GPa) alloy. The addition of Sn suppressed the double yielding verified on ternary alloy Ti25Ta25Nb.Electrochemical studies showed that stable passive oxide film was formed on the Ti25Ta25Nb3Sn surface and an increase of HDF adhesion and proliferation on alloy surface, indicating that the alloy is non-cytotoxic may provide a favorable material for biomedical applications. Results obtained showed that Ti25Ta25Nb3Sn alloy is indicated for biomedical applications.

1. Introduction

Titanium and its alloys have been extensively studied for biomedical applications for replacement hard tissues. However, the stress-shielding phenomenon is an important aspect that needs to be considered in the development of new titanium alloys for replacement hard tissues in biomedical applications. An alteration in the mechanical stimulus in the bone adjacent to the implant after implantation occurs principally due to the difference between the stiffness of the implant material as well as bone size, shape, and density [1].

Therefore, since 1990 s, new beta type titanium alloys formed by addition of non-toxic elements such as Nb, Ta, Zr, Mo and Sn with lower Young's modulus, high strength and corrosion resistance have been developed [2–13]. Two binary alloys systems, Ti–Nb [10, 14] and Ti–Ta [15–17], have been attracted attention as promising implant materials. Despite their higher corrosion resistance, the shape memory effect has been reported in these materials due to reversion α'' martensitic transformation to β phase. For the Ti–Nb alloys the martensitic transformation start temperature (M_S) increased with decreasing of niobium content in alloy [14]. Likewise, Ms temperature was below room temperature for Ti–40Ta (%at) alloy and Ms temperatures above 373 K for content less than Ti35Ta (%at).

The ternary alloy Ti25Ta25Nb formed by niobium and tantalum was proposed by Betrand *et al* [18, 19] and its cytotoxicity was evaluated by Cimpean *et al* [20]. This alloy exhibited higher corrosion resistance and biocompatibility. However, the double yielding effect in elastic region during tensile testing was observed. According Li *et al* [21] this phenomenon corresponds to the critical stress needed to induce α'' martensitic transformation to β phase and this low strength of the first yielding raises concern over the long-term use of implants made of these materials for biomedical applications. This effect can be suppressed by addition of alloying elements such as tin

(Sn). Tong *et al* [14] evaluated the influence of Sn addition in the Ti–Ta binary system. Ti–35Ta alloy exhibits a 'double yielding' phenomenon that disappeared for Ti30Ta5Sn alloy and only single yielding was observed. Based in these researches, we propose a new quaternary alloy, Ti25Ta25Nb3Sn, formed by the addition of Sn to initial composition of Ti25Ta25Nb ternary alloy. In this study, the crystalline phase formation, mechanical properties, corrosion resistance and biocompatibility was evaluated.

2. Experimental procedure

The ternary alloy Ti25Ta25Nb and new alloy quaternary Ti25Ta25Nb3Sn (% wt) were produced from sheets of commercially pure titanium (Ti), tantalum (Ta), niobium (Nb) and tin (Sn). After weighing, the materials were put in water-cooled copper crucible inside arc melting furnace and the furnace was evacuated and purged with argon at least five times. For chemical homogenization of the alloy, ingots were remelted and homogenization heat treatment was carried-out in vacuum at 1000 °C for 24 h and furnace cooled. Then, they were cold worked by rotary swaging into bars with 10 mm of diameter. Finally, they were subject to a solution treatment at 950 °C for 2 h followed by quenching. Ti25Ta25Nb was processed the same way and it was used as control group in all tests.

The crystalline phases formed were evaluated by x-ray Diffraction (XRD) using a PANanalytical Empyrean diffractometer operated at an accelerating voltage of 40 kV, current of 40 mA with Cu Kα radiation. For optical microscopy (OM) analysis, samples were prepared according standard metallographic procedure. Samples were ground using silicon carbide (SiC) paper (#100 to #1200 grit), polished with clothes using colloidal silica and cleaned in ultrasonic bath with acetone prior to use. The microstructure of the etched samples (Kroll's reagent) was evaluated by using an optical microscope (Epiphot 4 Nikkon).

Mechanical behavior was characterized by tensile test in a Universal Testing Machine (MTS) according to ASTM E8M at a strain rate of 3 mm min^{-1} at room temperature with strain gage. Standard cylindrical samples with gage dimensions 6 mm diameter and 25 mm length were machined for each alloy. Elastic modulus, 0.2% offset yield strength and maximum strength were determined.

Electrochemical measurements were performed to evaluate corrosion resistance of Ti25Ta25Nb3Sn alloy. Electrochemical experiments were carried-out in a standard three electrode double wall glass cell containing fluorinated physiological serum (0.15 M NaCl + 0.03 M NaF (pH = 6.0)) at 37 °C. The working electrode was made of the titanium CP, Ti25Ta25Nb and Ti25Ta25Nb3Sn discs with 0.5 cm^2 exposed area. Potentiodynamic polarization studies were performed after 3 h exposure to solution. Curves were recorded using a potenciostat/galvanostat EG & G PAR-283 by a scan rate of 1 mV s^{-1} with E_{OC} ranging from −0.3 V until +3.0 V.

Biocompatibility of the alloy was evaluated due the addition of tin. Before cytotoxicity test, samples were sterilized by gamma irradiation. Human Dermal Fibroblast cells (HDF, Clonetics) were used in this study once fibroblast cell line are the major cellular constituent of fibrous connective tissue adjacent to implant. Prior to cell culture, fibroblasts cells were isolated of neonatal foreskin, stored during 4 d at −80 °C and thawed in a water bath at 37 °C prior to cell culture. HDF cells were suspended in DMEM/High glucose (Hyciclone) medium with 50 ml of fetal bovine serum (Sigma) supplement and 5 ml of Penicillin Strep (Sigma). The suspensions were added into culture flasks (75 cm^3) and they were incubated at 37 °C in 5% CO_2 atmosphere until cells reached 70% confluence changing the medium each 72 h. When the cell suspensions reached 70% confluence, 3 mL of trypsin 0.25% solution was added to detached the cells and this enzymatic reaction was arrested by addition of a trypsin neutralizer (0.5% fetal bovine serum in phosphate-buffered saline (PBS)) after few minutes. The cells were aspirated, transferred to flasks and centrifuged at 180 g for 7 min. The cell pellet was resuspended in the 5 mL PBS (0.5% fetal bovine serum in phosphate-buffered saline). The number of cell was determined using the Scepter Cell Counter (Millipore). Cells from passage fifth were used in the experiments.

Samples were placed in 42-well plates, washed with three times with sterile PBS and HDF cells were seeded at a density of 3×10^4 cells mL^{-1}. The adhered and proliferated fibroblasts cells were quantified 1, 4 and 7 d after seeding using a colorimetric assay using MTT (3-[4,5-dimethylthiazol]-2,5 diphenyl tetrazolium bromide) (Sigma, Aldrich). The substrates were transferred to a new 24-well plate and incubated in 10% MTT solution in PBS for 3 h at 37 °C under a 5% CO_2 atmosphere and then it was added a mixture of 10% Triton X-100 in MTT solvent, with agitation. The absorbance of the solution was measured at a wavelength of 570 nm and 690 nm using a spectrophotometer. Fibroblast morphology on Ti25T25Nb3Sn alloy was evaluated after 1 and 7 d of culture using SEM.

3. Results and discussion

Optical micrographs of the Ti25Ta25Nb3Sn alloy and Ti25Ta25Sn after solution treatment along the transversal section are shown in figures 1(a) and (b), respectively. Despite the different steps used during processing of ternary alloy Ti–25Ta–25Nb in our study, the microstructure was like obtained for Bertrand *et al* [18, 19] for

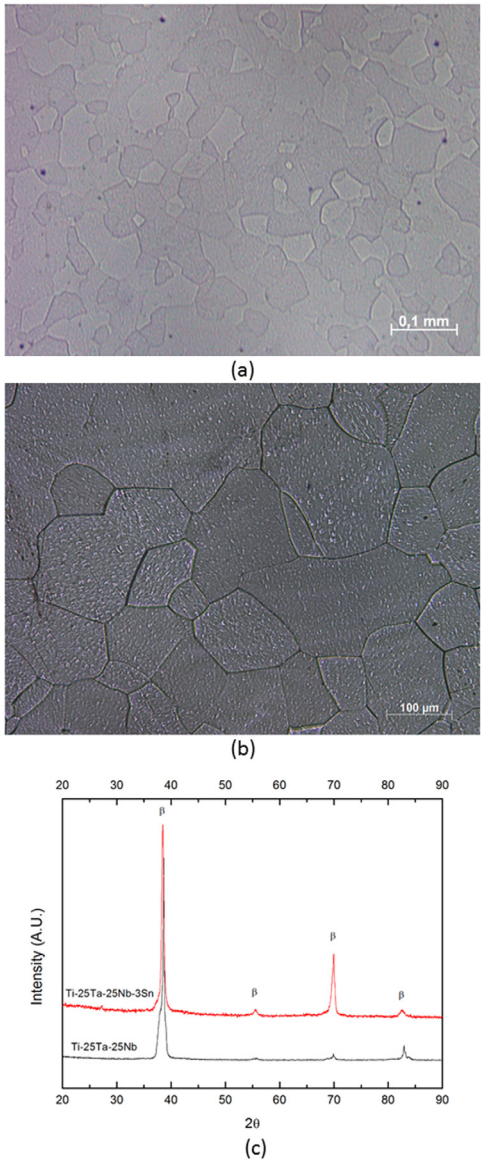

Figure 1. Optical micrographs of (a) Ti25Ta25Nb3Sn alloy (b) Ti25Ta25Nb alloy and (c) XRD patterns obtained for Ti25Ta25Nb3Sn and Ti25Ta25Nb alloys (treated at 950 °C for 2 h).

this alloy. For quaternary alloy Ti25Ta25Nb3Sn, the stabilization of beta phase was maintained with addition of Sn and changing in the grain size can be observed. The presence of β-phase was verified for either according XRD patterns (figure 1(c)) for both alloys, confirming the micrographs analysis. The obtaining of β Ti alloys for biomedical applications is viable due to low Young's modulus inhibiting the stress-shielding phenomena which occurs due to a mismatch in the stiffness of the biomedical material and bone tissue. Also, these alloys are easier to cold work when compared to $\alpha + \beta$ Ti alloys reducing the costs associated their processing [8].

Figure 2 shows the stress–strain curves obtained to Ti25Ta25Nb3Sn and compared with the curve obtained on ternary alloy Ti25Ta25Nb take as reference. The mechanical properties such as, tensile strength, Young's modulus and yield strength of Ti25Ta25Nb3Sn were compared with Ti CP and Ti6Al4V [22] from literature are showed in table 1. It was observed that the elastic modulus of Ti25Ta25Nb3Sn (65 GPa) was lower than Ti CP (110 GPa) and Ti6Al4V. The Young's modulus value was slightly higher than Ti25Ta25Nb alloy (55 GPa), however, the addition of Sn suppresses the transformation β to α'' verified to ternary alloy in the elastic deformation known as 'double yielding' [23]. A drop was observed in Ti25Ta25Nb3Sn, which can be attributed to stress-induced α'' formation during deformation [24].

Electrochemical tests evaluated the corrosion resistance of the alloy. Figure 3(a) shows the open circuit potential of the alloys as a function of exposure time in solution containing fluoridated physiological serum (0.15 M NaCl + 0.03 M NaF (pH = 6.0)) at 37 °C. OCP shift in the more noble direction and stabilized with time indicating the equilibrium between the formation and dissolution air-formed native oxide in these fluoride concentrations. The Ti25Ta25Nb shows the most positive OCP value, followed by Ti25Ta25Nb3Sn and Ti CP, i.e.

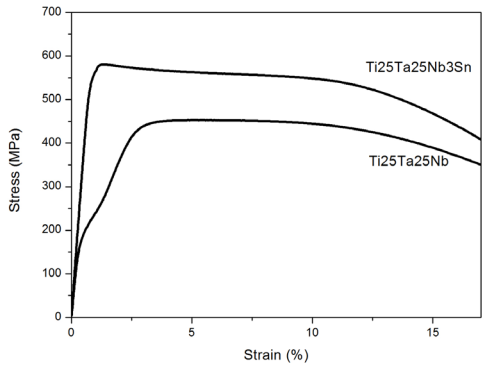

Figure 2. Representative stress–strain tensile curves of the Ti25Ta25Nb3Sn and Ti25Ta25Nb alloys.

Table 1. Mechanical properties of Ti CP, Ti6Al4V, Ti25Ta25Nb and Ti25Ta25Nb3Sn alloy.

	Ti CP	Ti6Al4V	Ti25Ta25Nb	Ti25Ta25Nb3Sn (this study)
LRT (MPa)	360	800–1100	530	583
σ_e (MPa)	310	930	210 (480) (double yielding)	567
E (GPa)	105–110	110–140	55	65

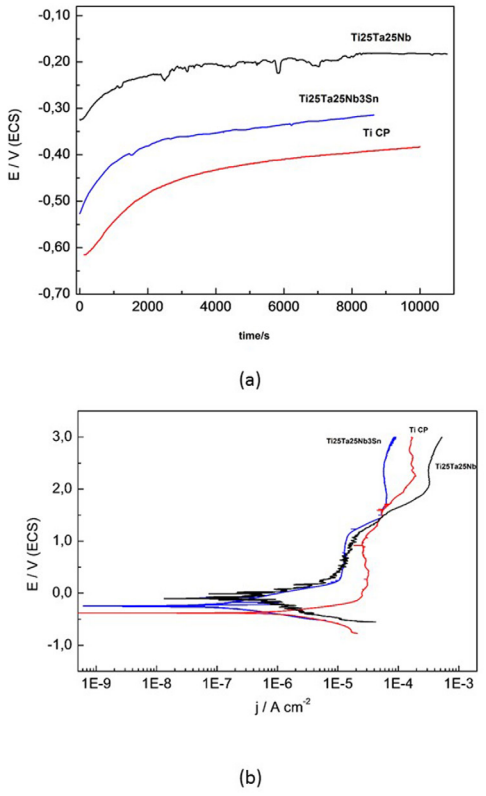

Figure 3. (a) Corrosion potential, E_{CORR} and (b) potentiodynamic polarization curves of Ti25Ta25Nb3Sn, Ti25Ta25Nb and CP Ti.

Ti25Ta25Nb > Ti25Ta25Nb3Sn >Ti CP. These values were used in potentiodynamic polarization tests to evaluate corrosion resistance.

Potentiodynamic polarization curves are shown in figure 3(b). It can be observed that Ti CP, Ti25Ta25Nb and Ti25Ta25Nb3Sn were spontaneously passive upon anodic polarization. However, Ti25Ta25Nb exhibited continuous increase in current density due to the breaking of the passive film. Similar results were observed by Karthega *et al* [25] for Ti29Nb13Ta4.6Zr (TNTZ) alloy in Hank's solution. According these studies, this behavior probably occurred due to dissolution of any one of the alloying elements. In our study, the addition of Sn resulted in the decreasing in passive current density which indicate an increase of their corrosion protective ability due to formation of protective film. The corrosion potential (E_{corr}), corrosion current density (i_{corr}) and passive current

Table 2. Main electrochemical parameters in fluoridated physiological serum (0.15 M NaCl + 0.03 M NaF (pH = 6.0)) at 37 °C.

	E_{OC} (mV)	E_{corr} (V)	J_{corr} (A cm^{-2})	J_{pass} (μA cm^{-2})
Ti-CP	−390	−380	1.4×10^{-6}	26
Ti25Ta25Nb3Sn	−310	−240	1.9×10^{-7}	13
Ti25Ta25Nb	−180	−130	6.7×10^{-7}	14

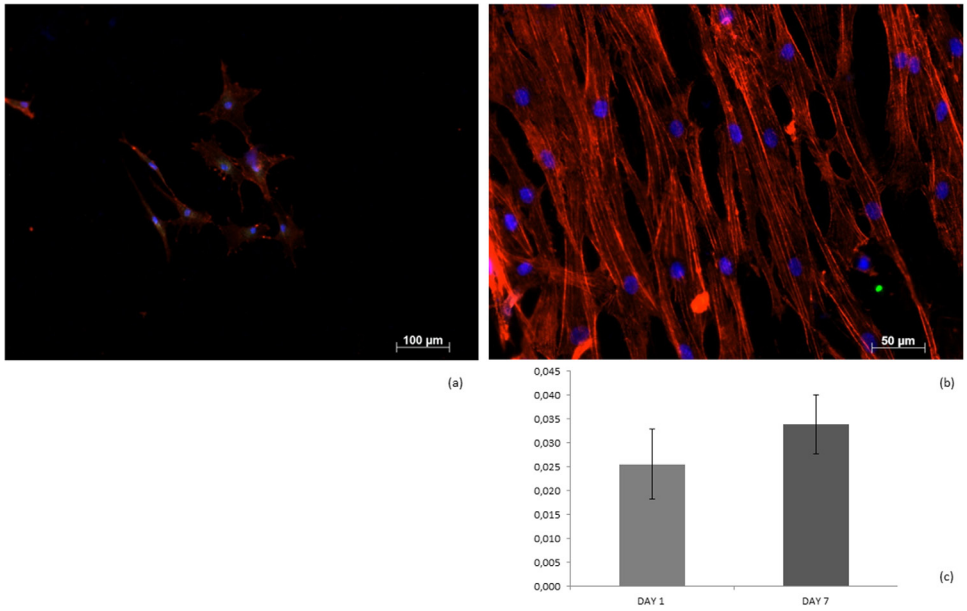

Figure 4. Fluorescence microscopy images of HDF cells after (a) 1 and (b) 7 d of culture on alloy surface (c) results from MTT assay indicating cell viability.

density (i_{pass}) of Ti CP, Ti25Ta25Nb and Ti25Ta25Nb3Sn are showed in table 2. Thus, this alloy shows a potential for biomedical applications due to high corrosion resistance.

The results from cell studies indicate an increase in HDF adhesion and proliferation on alloy surfaces after 7 d of culture (figures 4(a) and (b)). This indicates that alloy provides a favorable surface for enhanced adhesion and proliferation of HDF cells and does not have any cytotoxic effect. Further, the elongated morphology of the cells after 7 d elicits increased cell coverage and may activate additional focal adhesions, thus resulting in enhanced HDF cell functionality. MTT assay was used to evaluate the cytotoxicity of the alloy from the analysis of cell viability. MTT assay results (figure 4(c)) indicated the viability of HDF cells after 7 d of culture on alloy surface. These findings are in agreement with studies about cytotoxicity for others alloys previously published [15, 26–28] and they showed clearly the viability of this alloy for biomedical applications due to their good biocompatibility.

4. Conclusions

In the present study, the effect of Sn addition on properties of the Ti25Ta25Nb alloy was evaluated. New quaternary alloy (Ti25Ta25Nb3Sn) exhibited excellent bulk properties such as high strength and low elastic modulus. Besides, the addition of Sn suppressed the double yielding verified on Ti25Ta25Nb alloy. These results are important in load bearing applications, such as orthopedic applications. Electrochemical studies showed that stable passive oxide film was formed. Also, results showed an increase of HDF adhesion and proliferation on alloy surface, indicating that the alloy in non-cytotoxic may provide a favorable material for biomedical applications.

Acknowledgment

This work was supported by CAPES (Coordenação de Aperfeiçoamento de Pessoal de Nível Superior).

References

[1] Sumner D R 2015 Long-term implant fixation and stress-shielding in total hip replacement *J. Biomech.* **48** 797–800
[2] Escada A L A, Machado J P B, Schneider S G, Rezende M C R A and Alves Claro A P R 2011 Biomimetic calcium phosphate coating on Ti–7.5 Mo alloy for dental application *J. Mater. Sci., Mater. Med.* **22** 2457–65

[3] Chen X, Li Y, Hodgson P D and Wen C 2011 *In vitro* behavior of human osteoblast-like cells ($SaOS_2$) cultured on surface modified titanium and titanium–zirconium alloy *Mater. Sci. Eng.* C **31** 1545–52
[4] Rosalbino F, Maccio D, Scavino G and Saccone A 2012 *In vitro* corrosion behaviour of Ti–Nb–Sn shape memory alloys in Ringer's physiological solution *J. Mater. Sci., Mater. Med.* **23** 865–71
[5] Rezende M C R A, Alves A P R, Codaro E N and Dutra C A M 2007 Effect of commercial mouthwashes on the corrosion resistance of Ti–10Mo experimental alloy *J. Mater. Sci., Mater. Med.* **18** 149–54
[6] Alves A P R, Santana F A, Rosa L A A, Cursino S A and Codaro E N 2004 A study on corrosion resistance of the Ti–10Mo experimental alloy after different processing methods *Mater. Sci. Eng.* C **24** 693–6
[7] Niemeyer T C, Grandini C R, Pinto L M C, Angelo A C D and Schneider S G 2009 Corrosion behavior of Ti–13Nb–13Zr alloy used as a biomaterial *J. Alloys Compd.* **476** 172–5
[8] Ozan S, Lin J, Li Y, Ipek R and Wen C 2015 Development of Ti–Nb–Zr alloys with high elastic admissible strain for temporary orthopedic devices *Acta Biomater.* **20** 176–87
[9] Lin D J, Chuang C C, Lin J H C, Lee J W, Ju C P and Yin H S 2007 Bone formation at the surface of low modulus Ti–7.5 Mo implants in rabbit femur *Biomaterials* **28** 2582–9
[10] Afonso C R M, Aleixo G T, Ramirez A J and Caram R 2007 Influence of cooling rate on microstructure of Ti–Nb alloy for orthopedic implants *Mater. Sci. Eng.* C **27** 908–13
[11] Júnior M, Severino J R, Nogueira R A, Araújo R O D, Donato T A G, Arana-Chavez V E, Alves Claro A P R, Moraes J C S and Grandini C R 2011 Preparation and characterization of Ti–15Mo alloy used as biomaterial *Mater. Res.* **14** 107–12
[12] Chaves J M, Escada A L A, Rodrigues A D and Alves Claro A P R 2016 Characterization of the structure, thermal stability and wettability of the TiO_2 nanotubes growth on the Ti–7.5 Mo alloy surface *Appl. Surf. Sci.* **370** 76–82
[13] da Silva L M, Claro A P R A, Donato T A G, Arana-Chavez V E, Moraes J C S, Buzalaf M A R and Grandini C R 2011 Influence of heat treatment and oxygen doping on the mechanical properties and biocompatibility of titanium–niobium binary alloys *Artif. Organs* **35** 516–21
[14] Tobe H, Kim H Y, Inamura T, Hosoda H, Nam T H and Miyazaki S 2013 Effect of Nb content on deformation behavior and shape memory properties of Ti–Nb alloys *J. Alloys Compd.* **577** S435–8
[15] Capellato P, Escada A L A, Popat K C and Alves Claro A P R 2014 Interaction between mesenchymal stem cells and Ti–30Ta alloy after surface treatment *J. Biomed. Mater. Res.* A **102** 2147–56
[16] Capellato P, Riedel N A, Williams J D, Machado J P B, Popat K C and Alves Claro A P 2013 Surface modification on Ti–30Ta alloy for biomedical application *Engineering* **5** 707–13
[17] Zhou Y L, Niinomi M and Akahori T 2004 Decomposition of martensite α''during aging treatments and resulting mechanical properties of Ti–Ta alloys *Mater. Sci. Eng.* A **384** 92–101
[18] Bertrand E, Castany P and Gloriant T 2013 Investigation of the martensitic transformation and the damping behavior of a superelastic Ti–Ta–Nb alloy *Acta Mater.* **61** 511–8
[19] Bertrand E, Gloriant T, Gordin D M, Vasilescu E, Drob P, Vasilescu C and Drob S I 2010 Synthesis and characterisation of a new superelastic Ti–25Ta–25Nb biomedical alloy *J. Mech. Behav. Biomed. Mater.* **3** 559–64
[20] Cimpean A, Mitran V, Ciofrangeanu C M, Galateanu B, Bertrand E, Gordin D M, Iordachescu D and Gloriant T 2012 Osteoblast cell behavior on the new beta-type Ti–25Ta–25Nb alloy *Mater. Sci. Eng.* C **32** 1554–63
[21] Li S J, Cui T C, Hao Y L and Yang R 2008 Fatigue properties of a metastable β-type titanium alloy with reversible phase transformation *Acta Biomater.* **4** 305–17
[22] Nalla R K, Altenberger I, Noster U, Liu G Y, Scholtes B and Ritchie R O 2003 On the influence of mechanical surface treatments—deep rolling and laser shock peening—on the fatigue behavior of Ti–6Al–4V at ambient and elevated temperatures *Mater. Sci. Eng.* A **355** 216–30
[23] Tong Y X, Guo B, Zheng Y F, Chung C Y and Ma L W 2011 Effects of Sn and Zr on the microstructure and mechanical properties of Ti–Ta-based shape memory alloys *J. Mater. Eng. Perform.* **20** 762–6
[24] Hanada S, Masahashi N and Jung T K 2013 Effect of stress-induced α'' martensite on Young's modulus of β Ti–33.6Nb–4Sn alloy *Mater. Sci. Eng.* A **588** 403–10
[25] Karthega M, Raman V and Rajendran N 2007 Influence of potential on the electrochemical behaviour of β titanium alloys in Hank's solution *Acta Biomater.* **3** 1019–23
[26] Capellato P, Smith B S, Popat K C and Alves Claro A P R 2012 Fibroblast functionality on novel Ti30Ta nanotube array *Mater. Sci. Eng.* C **32** 2060–7
[27] Zhang X, Li Z, Yuan X, Cui Z, Bao H, Li X, Lui Y and Yang X 2013 Cytotoxicity and antibacterial property of titanium alloy coated with silver nanoparticle-containing polyelectrolyte multilayer *Mater. Sci. Eng.* C **33** 2816–20
[28] Zhang R F, Qiao L P, Qu B, Zhang S F, Chang W H and Xiang J H 2015 Biocompatibility of micro-arc oxidation coatings developed on Ti6Al4V alloy in a solution containing organic phosphate *Mater. Lett.* **153** 77–80